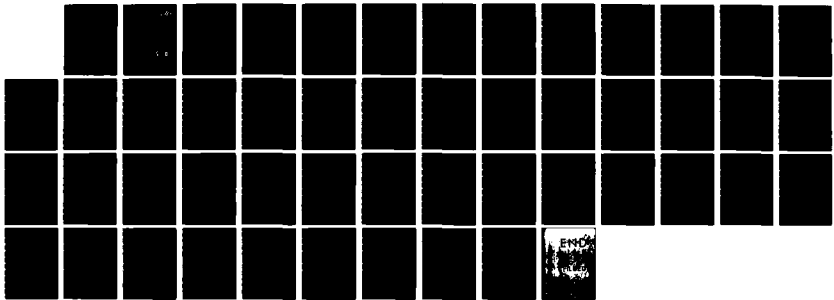
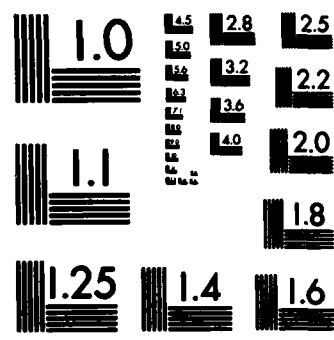


HD-A133 762 MECHANICAL RESPONSE OF MATERIALS WITH PHYSICAL DEFECTS 1/1
PART 3 A MATERIAL. (U) LEHIGH UNIV BETHLEHEM PA INST OF
FRACTURE AND SOLID MECHANICS. G C SIH ET AL. JUL 83
UNCLASSIFIED IFSM-83-117 AFOSR-TR-83-0871 AFOSR-82-0194 F/G 20/11 NL



EMC



MICROCOPY RESOLUTION TEST CHART
NATIONAL BUREAU OF STANDARDS-1963-A

AD - A133762

AFOSR-TR- 83-0871

IFSM-83-117



MECHANICAL RESPONSE OF MATERIALS
WITH PHYSICAL DEFECTS
PART 3: A MATERIAL TESTING
PROGRAM FOR SIZE AND RATE EFFECTS

BY

G. C. SIH AND P. MATIC

FINAL TECHNICAL REPORT

AFOSR-82-0194

JULY 1983

DTIC
ELECTED
OCT 20 1983
S D

Approved for public release;
distribution unlimited.

DTIC FILE COPY

AIR FORCE OFFICE OF SCIENTIFIC RESEARCH

BOLLING AIR FORCE BASE, D.C. 20332

00 10 10 208

UNCLASSIFIED

REPORT DOCUMENTATION PAGE

STANDARD FORM
12 JAN 72
BEFORE COMPLETING

RECIPIENT'S CATALOG NUMBER

1. REPORT NUMBER AFOSR-TR-83-0871		2. GOVT ACCESSION NO. AD-A133762	3. DATES COVERED 01 JAN 82-30 MAR 83
4. TITLE (and Subtitle) MECHANICAL RESPONSE OF MATERIALS WITH PHYSICAL DEFECTS PART 3: A MATERIAL TESTING PROGRAM FOR SIZE AND RATE DEFECTS		5. TYPE OF REPORT & PERIOD COVERED FINAL: 01 JAN 82-30 MAR 83	
7. AUTHOR(s) G C SIH P MATIC		6. PERFORMING ORG. REPORT NUMBER IFSM-83-117	
9. PERFORMING ORGANIZATION NAME AND ADDRESS LEHIGH UNIVERSITY BETHLEHEM, PA 18015		10. PROGRAM ELEMENT, PROJECT, TASK AREA & WORK UNIT NUMBERS 61102F 2307/B2	
11. CONTROLLING OFFICE NAME AND ADDRESS AFOSR/NA Bolling AFB DC 20332		12. REPORT DATE July 1983	
14. MONITORING AGENCY NAME & ADDRESS (if different from Controlling Office)		13. NUMBER OF PAGES 45	
		15. SECURITY CLASS. (of this report) UNCLASSIFIED	
		16a. DECLASSIFICATION/DOWNGRADING SCHEDULE	
16. DISTRIBUTION STATEMENT (of this Report) Approved for public release; distribution unlimited.			
17. DISTRIBUTION STATEMENT (of the abstract entered in Block 20, if different from Report)			
18. SUPPLEMENTARY NOTES			
19. KEY WORDS (Continue on reverse side if necessary and identify by block number) Yielding Fracture Crack growth Material damage Strain energy density Nonlinear response			
20. ABSTRACT (Continue on reverse side if necessary and identify by block number) A fundamental problem of structural analysis is the prediction of the final failure mode. Traditional approaches to the extreme forms of failure, i.e. plastic collapse and fracture instability, invoke a particular failure criterion to address one assumed failure mode. The appearance of the other mode is precluded by such an approach.			
A criterion is presented which addresses both macrocrack propagation and local changes in material properties using strain energy density. The damage state of			

~~UNCLASSIFIED~~

the material at a particular instant of its load history is assumed to be governed by loading versus unloading behavior of the material's constitutive law. Macrocrack instability is assumed to occur when the size of the core region around the crack tip exceeds the predicted growth increment. This core region is defined by the closed contour of constant strain energy density equal to the maximum value addressed by the constitutive law. Crack growth increments occur in the direction of minimum strain energy density. The length of the crack growth increment is governed by the relative toughness of the material in the direction of propagation.

The criterion is applied to a set of three cylindrical test specimens. using the finite element method. A brittle-elastic material is used to demonstrate the criterion. Damage at the continuum scale for this type of material is treated in terms of a local reduction in the elastic modulus. The specimens are all geometrically similar, with lengths equal to 4 times the radii. They vary in size with radii of 0.3", 0.4", and 0.5", respectively. Uniaxial stress is applied to the ends of each specimen. A 0.1" radius crack, perpendicular to the specimen axis, is assumed to coincide with the onset of specimen nonlinearity. Using constant applied stress increments, a series of damage/crack propagation analyses is performed using the strain energy density criterion. Specimen instability loads are predicted from the crack instability condition.

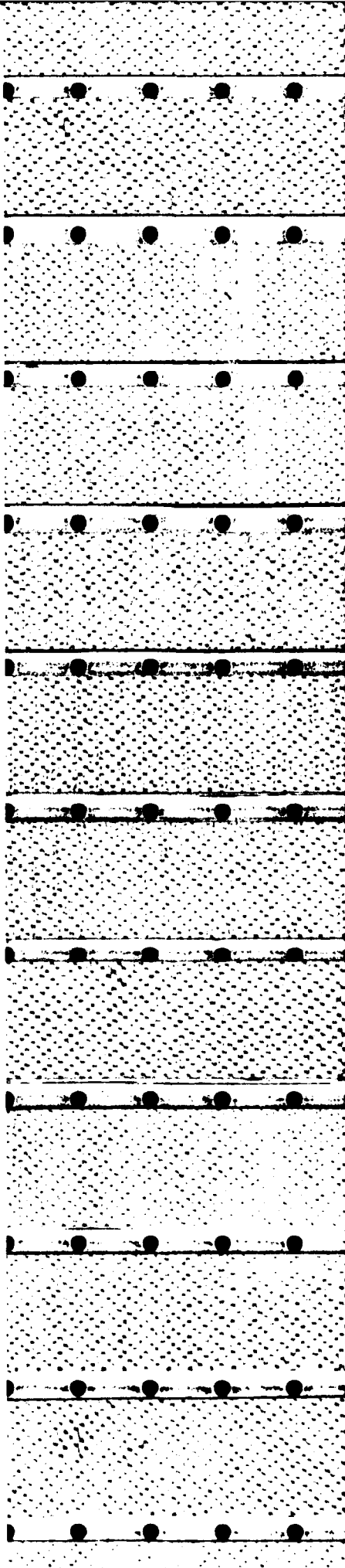
Increasing specimen size is shown to lead to less crack growth prior to instability. Load-displacement data was converted to a strain-strain representation for each of the specimens. The influence of specimen size and subsequent material inhomogeneity inside the specimen are evident in the different responses obtained for each specimen from the same constitutive law used as input for the analysis. The scaling of specimen size to crack growth is demonstrated using the strain energy density factor.

Accession For	
NTIS GRA&I	<input checked="" type="checkbox"/>
DTIC TAB	<input type="checkbox"/>
Unannounced	<input type="checkbox"/>
Justification	
By _____	
Distribution/	
Availability Codes	
Dist	Avail and/or Special
R	



~~UNCLASSIFIED~~

SECURITY CLASSIFICATION OF THIS PAGE (If Different From Document)



MECHANICAL RESPONSE OF MATERIAL WITH PHYSICAL DEFECTS

3: A MATERIAL TESTING PROGRAM FOR SIZE AND RATE EFFECTS

by

G. C. Sih and P. Matic

Institute of Fracture and Solid Mechanics

Lehigh University

July 1983

AIR FORCE OFFICE OF SCIENTIFIC RESEARCH (AFSC)
NOTICE OF TRANSMITTAL TO DTIC
This technical report has been reviewed and is
approved for public release IAW AFR 190-12.
Distribution is unlimited.

MATTHEW J. KERPER
Chief, Technical Information Division

ABSTRACT

A fundamental problem of structural analysis is the prediction of the final failure mode. Traditional approaches to the extreme forms of failure, i.e. plastic collapse and fracture instability, invoke a particular failure criterion to address one assumed failure mode. The appearance of the other mode is precluded by such an approach.

A criterion is presented which addresses both macrocrack propagation and local changes in material properties using strain energy density. The damage state of the material at a particular instant of its load history is assumed to be governed by loading versus unloading behavior of the material's constitutive law. Macrocrack instability is assumed to occur when the size of the core region around the crack tip exceeds the predicted growth increment. This core region is defined by the closed contour of constant strain energy density equal to the maximum value addressed by the constitutive law. Crack growth increments occur in the direction of minimum strain energy density. The length of the crack growth increment is governed by the relative toughness of the material in the direction of propagation. ↵

The criterion is applied to a set of three cylindrical test specimens using the finite element method. A brittle-elastic material is used to demonstrate the criterion. Damage at the continuum scale for this type of material is treated in terms of a local reduction in the elastic modulus. The specimens are all geometrically similar, with lengths equal to 4 times the radii. They vary in size with radii of 0.3", 0.4", and 0.5", respectively.

Uniaxial stress is applied to the ends of each specimen. A 0.1" radius crack, perpendicular to the specimen axis, is assumed to coincide with the onset of specimen nonlinearity. Using constant applied stress increments, a series of damage/crack propagation analyses is performed using the strain energy density criterion. Specimen instability loads are predicted from the crack instability condition.

Increasing specimen size is shown to lead to less crack growth prior to instability. Load-displacement data was converted to a strain-strain representation for each of the specimens. The influence of specimen size and subsequent material inhomogeneity inside the specimen are evident in the different responses obtained for each specimen from the same constitutive law used as input for the analysis. The scaling of specimen size to crack growth is demonstrated using the strain energy density factor.

INTRODUCTION

The prediction of structural component failure in the presence of micro-damage and macrocrack propagation is an area of fundamental interest which is not well understood. The traditional approach to failure prediction has been to apply separate and distinct criteria to different energy dissipative processes (e.g. plasticity versus macrocrack propagation). In contrast, this investigation has been directed toward the development of a criterion, based on strain energy density, which treats both microdamage and macrocrack propagation together in a consistent manner.

The utility of any criterion used to predict structural component behavior and failure lies in its ability to address a wide range of loading conditions and structural applications. In practice, the principles of continuum mechanics are used to define the quantities which govern elastic and elastic-plastic material behavior. Unfortunately, it is a commonly observed fact that the size of a material test specimen, the independent variable of loading, and the rate at which the loading proceeds may significantly alter the observed behavior of a material. This is present across scale boundaries, from global response to microstructural appearances to dislocation movement. The use of any such test results are subject to question if no meaningful interpretation is available to relate a particular specimen behavior to the material behavior in the component itself. For any material test to be complete, the evaluation of material constants and material behavior parameters must be approached with a recognition of the role that specimen size and loading rate effects do indeed have on the specimen, and will subsequently have, when applied to analytic or numerical modeling.

It is the purpose of this investigation to propose a material testing procedure which addresses these aspects of material behavior. The response of three uniaxial test specimens, each of a different size, will be calculated using finite element procedures and the strain energy density criterion. The material constitutive relation and load increment will be fixed for all three specimens. In addition to the influence of specimen size on global nonlinear behavior, the numerical prediction of crack instability parameters will be presented along with results useful in estimating the size of specimens which will fail in an ideally brittle manner.

STRAIN ENERGY DENSITY THEORY OF MICRODAMAGE AND MACROCRACK PROPAGATION

Strain Energy Density Theory, as proposed by Sih [1,2] and applied to microdamage by Sih and Matic [3,4], makes use of the energy state of the material and its associated material properties. The theory predicts both the onset, development, and intensity of microdamage as well as the direction and magnitude of macrocrack growth increments. The treatment of both macro- and microdamage by one quantity is in contrast to traditional failure criteria which select the failure mechanism prior to analysis.

The value of strain energy density function $\Delta W/\Delta V$ at any two points of a solid body subjected to load, in the absence of singularities, will generally be on the same order of magnitude. The presence of strain energy concentrations or singularities, however, will produce regions of intense deformation. In such regions the constitutive equations used in the analysis of the body may be inadequate to describe the material behavior at the continuum scale. In the case of a well defined macrocrack, the singularity associated with the crack tip results in a "core region", necessitating the investigation of material elements at a finite distance from the crack tip, where the techniques of continuum stress and damage analysis remain valid.

The strain energy density field in the neighborhood of the crack tip has the form

$$\frac{\Delta W}{\Delta V} = \frac{1}{r} [S(a, \theta, \text{material properties})] + \text{nonsingular terms} \quad (1)$$

where r is the radial distance from the crack tip, a is the crack length parameter, θ is the angular position coordinate, and the function S is the

strain energy factor which is the coefficient of the r^{-1} singularity exhibited by the energy density field. In the case of linear, homogeneous and isotropic elasticity, the strain energy density factor can be expressed in terms of the stress intensity factors k_1 , k_2 and k_3 as

$$S = a_{11}k_1^2 + a_{12}k_1k_2 + a_{22}k_2^2 + a_{33}k_3^2 \quad (2)$$

where the a_{ij} ($i,j = 1,2,3$) are functions of the elastic shear modulus, Poisson's ratio, and angle θ . The stress intensity factors take the form

$$k_j = c_j \sigma_{kl} \sqrt{a} \quad (3)$$

where the c_j are geometry and load dependent, and σ_{kl} is the remote applied stress. For more common cases where microdamaged material is near the crack tip, this lack of homogeneity precludes a one parameter characterization of the crack tip. Furthermore, the present lack of an adequate analytical treatment of the crack tip requires a numerical approach to the region.

A description of the continuum behavior of a material must address both the microdamage and macrocrack propagation processes. Traditionally, the global load-displacement response of a uniaxial tensile specimen has been used to measure the elastic modulus and Poisson's ratio of a nonlinear isotropic material. This is accomplished by defining the true stress and true strain, referenced to cross sectional specimen area and specimen length. The true stress - true strain response of the material remains valid for as long as the specimen exhibits material homogeneity. The irreversible processes which develop, however, inevitably produce material inhomogeneity within the specimen. This invalidates the measurement of continuum prop-

erties from the specimen in the rigorous sense.

The translation of the aggregate continuum behavior within the specimen to the global specimen response, in light of specimen inhomogeneity, is a question fundamental to any type of structural behavior prediction. To investigate this in a consistent manner requires a knowledge of the strain energy density behavior at the continuum scale. If one assumes that an appropriate true stress - true strain curve characterizing an isotropic material at the continuum scale is available, the strain energy density at some point in the loading history is

$$\frac{\Delta W}{\Delta V} = \int_0^{\epsilon_k} \sigma d\epsilon \quad (4)$$

where σ is the true strain, and ϵ_k is some value of the true strain prior to specimen failure. For an assumed material response, such as in Figure 1, the true stress - true strain curve is assumed to be expressible by the relations

$$\sigma = E_1 \quad \sigma < \sigma_y \quad (5)$$

$$\frac{\sigma}{\sigma_y} = \left(\frac{\epsilon}{\epsilon_y} \right)^n \quad \sigma > \sigma_y \quad . \quad (6)$$

The strain energy density obtained from such a true stress - true strain relation will be

$$\begin{aligned} \left(\frac{\Delta W}{\Delta V} \right) &= \int_0^{\epsilon_y} \sigma d\epsilon + \int_{\epsilon_y}^{\epsilon_k} \sigma d\epsilon \\ &= \left(\frac{\Delta W}{\Delta V} \right)_y + \frac{\sigma_y}{E_1} \frac{\epsilon_k^{n+1} - \epsilon_y^{n+1}}{n+1} \\ &= \frac{1}{2} \frac{\sigma_y^2}{E_1} + \frac{\sigma_y}{E_1} \frac{\epsilon_k^{n+1} - \epsilon_y^{n+1}}{n+1} \quad . \quad (7) \end{aligned}$$

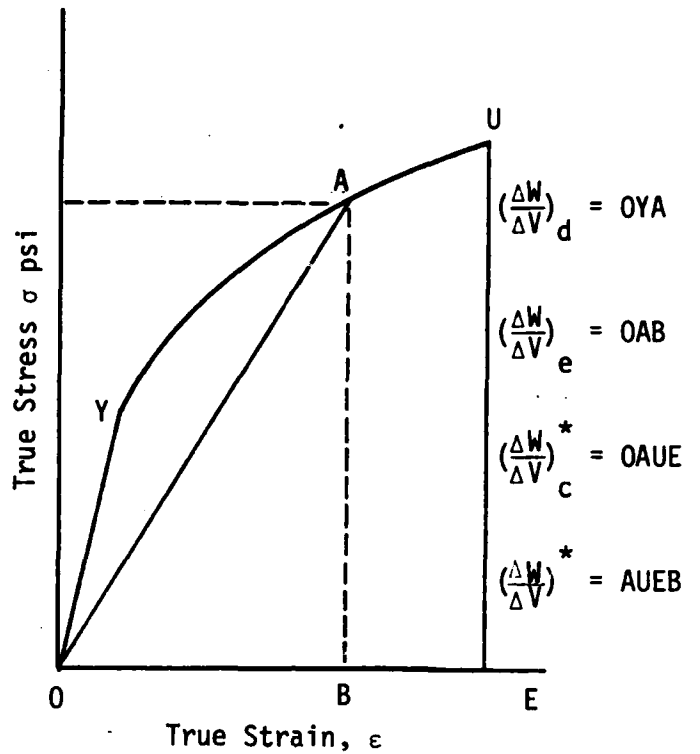


Figure 1 - Strain Energy Density Definitions From Uniaxial True Stress - True Strain Curve

The onset of yielding, or the dissipation of energy through micro-damage, will occur when

$$\left(\frac{\Delta W}{\Delta V}\right) = \left(\frac{\Delta W}{\Delta V}\right)_y . \quad (8)$$

For subsequent loading

$$\left(\frac{\Delta W}{\Delta V}\right) > \left(\frac{\Delta W}{\Delta V}\right)_y , \quad (9)$$

and the energy dissipated, in the material element, i.e. $(\Delta W/\Delta V)_d$, corresponds to the area OYA on the stress-strain curve. Any material elements which are microdamaged and lie on the subsequent fracture path of the macrocrack

will be less resistant to fracture by the amount $(\Delta W/\Delta V)_d$. Hence, the value of critical strain energy density is relative to the energy already dissipated, according to the relation

$$\left(\frac{\Delta W}{\Delta V}\right)_c^* = \left(\frac{\Delta W}{\Delta V}\right)_c^* - \left(\frac{\Delta W}{\Delta V}\right)_d . \quad (10)$$

If the crack propagates into undamaged material, then clearly no microdamage is present to weaken the material, and

$$\left(\frac{\Delta W}{\Delta V}\right)_c^* = \left(\frac{\Delta W}{\Delta V}\right)_c . \quad (11)$$

The relation of the relative critical value of $(\Delta W/\Delta V)_c^*$ to the critical value $(\Delta W/\Delta V)_c$ is given by the respective areas OAUE and OYAUE on the schematic stress-strain curve, as seen in Figure 1, for loading to an arbitrary point A.

For unloading, it will be assumed in this report that the material behaves in a pseudo-linear elastic manner by unloading along line A0 back to the origin. The advantages of such a material model lie in the ability to investigate fundamental aspects of global stiffness of the specimen as compared to the reduced local stiffness (i.e. the reduced elastic modulus) at the continuum scale. It should be evident that for each value of strain energy density

$$\left(\frac{\Delta W}{\Delta V}\right)_i > \left(\frac{\Delta W}{\Delta V}\right)_y \quad (12)$$

their corresponds a value of secant elastic modulus (or reduced modulus)

$$E_i < E_1 \quad (13)$$

since yielding of the material is a continuous process, the secant modulus

will assume a spectrum of values throughout the load history. Furthermore, the interaction of macro and microdamage may be addressed in a more meaningful way when the damage processes qualitatively produce the same types of effects at their respective scales. The fundamental concepts of the theory remain applicable to a wide variety of materials and dissipative processes.

At any point A on the stress-strain curve, the recoverable elastic strain energy density will be area OAB. The additional energy required to reach the critical value $(\Delta W/\Delta V)_c$ may be defined as $(\Delta W/\Delta V)^*$, which corresponds to the area AUEB under the curve. The relative critical strain energy density may then be expressed as

$$\left(\frac{\Delta W}{\Delta V}\right)_c^* = \left(\frac{\Delta W}{\Delta V}\right)_e + \left(\frac{\Delta W}{\Delta V}\right)^*. \quad (14)$$

The fundamental hypotheses of the strain energy density theory applied to both fracture and yielding may be stated as follows:

(I) Yielding and fracture are assumed to coincide with the locations of relative maximum $(\Delta W/\Delta V)_{\max}$ and relative minimum $(\Delta W/\Delta V)_{\min}$ of the strain energy density function.

(II) Yielding and fracture are assumed to occur when $(\Delta W/\Delta V)_{\max}$ and $(\Delta W/\Delta V)_{\min}$ reach their respective critical values, $(\frac{\Delta W}{\Delta V})_y$ and $(\frac{\Delta W}{\Delta V})_c$.

(III) The local response of the material, to either an increase or decrease in applied load, is governed by the amount of strain energy dissipated by smaller scale processes within a continuum material volume. This dissipation occurs within the range $(\Delta W/\Delta V)_y \leq (\Delta W/\Delta V) \leq (\Delta W/\Delta V)_c$.

(IV) The amount of each incremental of crack growth in fracture, say r_j , is given by

$$\left(\frac{\Delta W}{\Delta V}\right)_c^* = \frac{s_j^*}{r_j} \quad (15)$$

as shown in Figure 2. The * superscript takes into account the influence of smaller scale damage on the local material toughness and on the nature of the singular energy field as influenced by the current state of the material.

From the amount of incremental crack growth, the strain energy density factor at each increment, say s_1, s_2, \dots, s_j , is calculated from the relation

$$\left(\frac{\Delta W}{\Delta V}\right)_c = \frac{s_1}{r_1} = \frac{s_2}{r_2} = \dots = \frac{s_j}{r_j} \quad (16)$$

This is shown in Figure 3.

If the crack growth process leads to instability s_j/r_j approaches s_c/r_c , where s_c and r_c are material parameters.

The prediction of crack instability follows from an examination of the range of strain energy density magnitudes described by the constitutive law and its relation to the concept of the core region near the crack tip. For a given material constitutive law, consider the core region to be defined as the material volume enclosed by a surface of constant $\Delta W/\Delta V$ equal to the lowest value of $\left(\frac{\Delta W}{\Delta V}\right)_c^*$ calculated from the true stress - true strain curve of the material. Physically, this surface represents a volume of material for which the constitutive law is invalid in the strain energy density sense. The lowest value of $\left(\frac{\Delta W}{\Delta V}\right)_c^*$ physically corresponds to that state of the

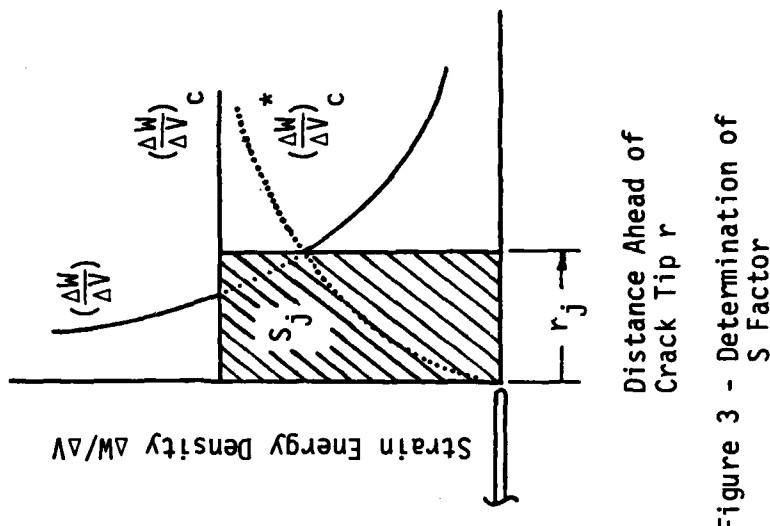


Figure 3 - Determination of S Factor

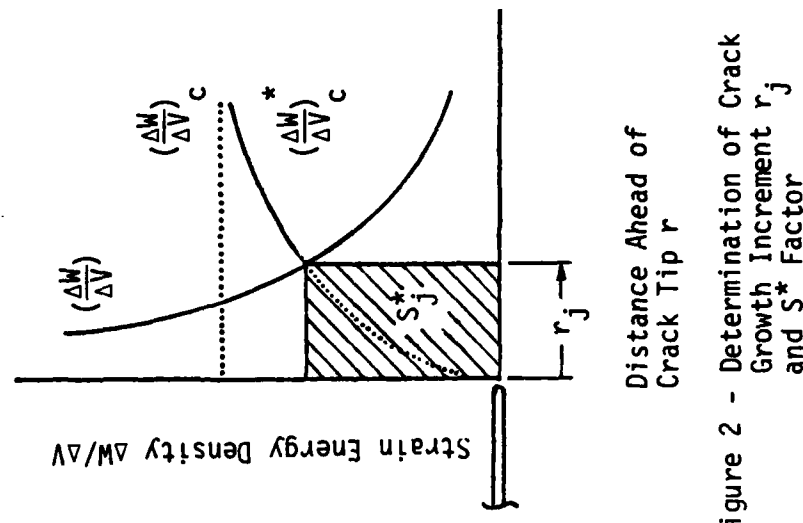


Figure 2 - Determination of Crack Growth Increment r_j and S^* Factor

material for which the material may no longer dissipate energy through smaller scale mechanisms should $\Delta W/\Delta V$ exceed $(\Delta W/\Delta V)_c^*$.

As described above, the intersection of $\Delta W/\Delta V$ and $(\Delta W/\Delta V)_c^*$ in the direction of crack propagation will govern the size of the crack growth increment according to Equation (15). Typically, the boundary of the core zone will lie within the increment of crack growth (Figure 4). That portion of stable crack growth, within the core region, proceeds into material unable to further dissipate energy through smaller scale mechanisms. The crack is momentarily destabilized in this region. The portion of the crack growth increment extending from the core region boundary out to the end of the increment, but still able to dissipate energy through small scale mechanisms, will locally stabilize the crack at its new length. This process repeats itself for subsequent stable crack growth increments.

As the crack grows in a stable manner, the core region will gradually increase in size while the size of the crack growth increments will also generally increase, though at a relatively slower lineal rate. (While it is assumed that the crack is situated and grows in such a manner, this discussion does not preclude situations where these growth increments may be attenuated due to structural geometry, load history, etc.) At some point, the size of the core region boundary in the direction of crack growth will reach or exceed the length of the crack growth increment itself (Figure 5). In the absence of any additional dissipative capability of material in this increment, it will be assumed that the crack will not arrest at the end of such an increment. This, of course, corresponds to crack instability in the

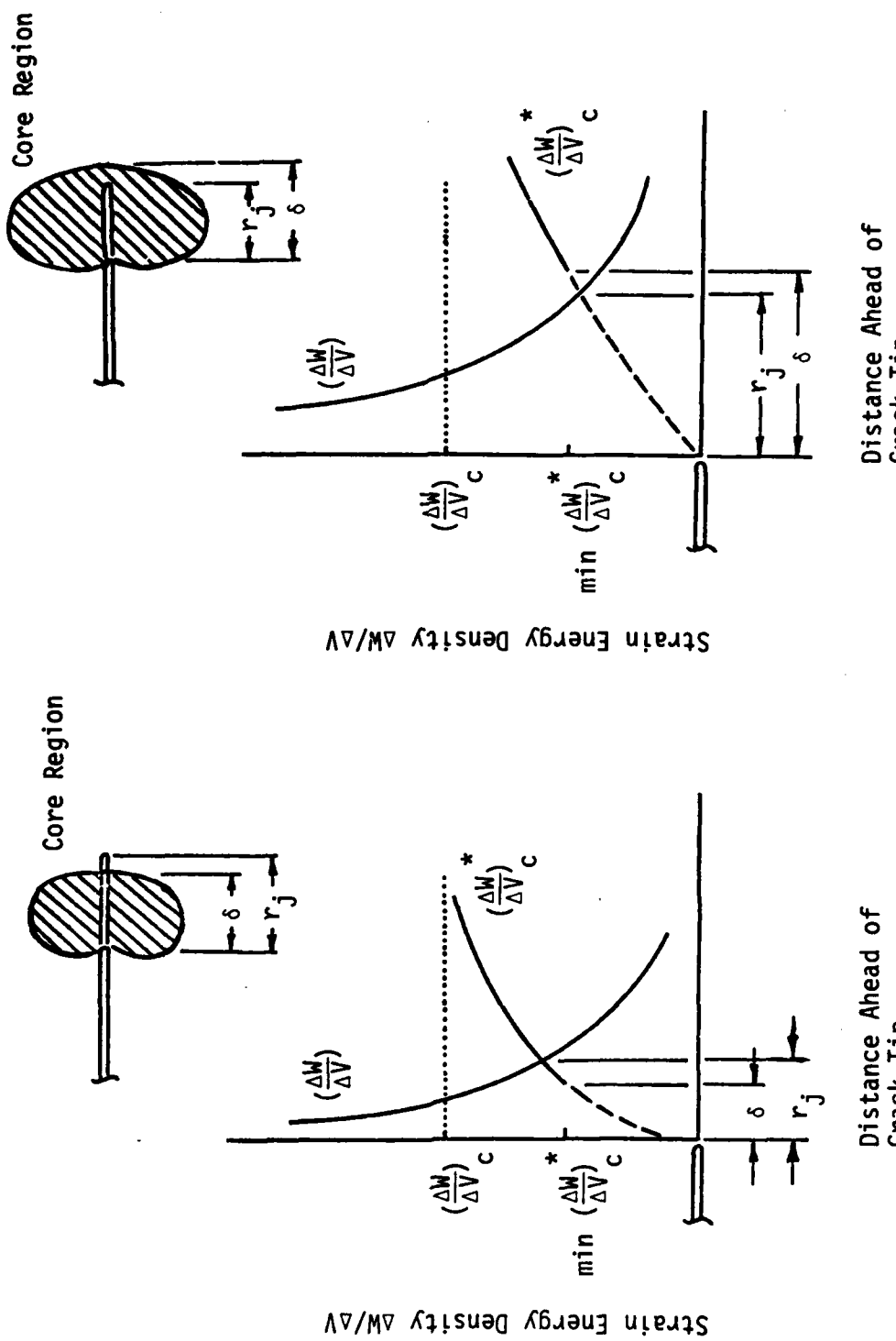


Figure 4 - Stable Crack Growth Increment

Figure 5 - Crack Growth Increment at Crack Instability

global sense. If the boundary of the core region happens to lie outside the increment length, overload of the crack results. If, at some point in the crack trajectory, the structural geometry, load history, or other factors cause the relative size of the core region to diminish below the crack increment size, crack arrest is assumed to occur, and stable growth analysis could proceed.

MATERIAL TESTING CONSIDERATIONS ADDRESSING SPECIMEN SIZE AND LOADING RATE EFFECTS

As mentioned above, the continuum analysis of structures is dependent on the ability of a simple test (or a set of simple tests) to characterize the material constants and material behavior parameters which appear in the constitutive law of the material. It is important, at this point, to clearly distinguish between these two terms as they apply to this investigation. Specifically, a "material constant" will refer to a parameter which is observed to be independent of the conditions and specifics of the test used to measure its value. A "material behavior parameter" will refer to a quantity which is unique to the conditions and the specifics of the test used to measure its value. In the case of linear, isotropic elasticity, two independent material constants (e.g. Young's modulus and the shear modulus) are required to characterize the material behavior. In the case of nonlinear, isotropic elasticity or elastic-plastic deformation, material constants alone are inadequate to describe the material behavior. Typically, one or more material parameters (e.g. strain hardening exponent) are introduced to account for the observed nonlinearity of the material. Such nonlinearity is often quite sensitive to the method used to obtain its value.

Nonlinear response of material test specimens to applied load is associated with the energy dissipative processes within the material. Plasticity and microcracking are two examples of this. The precise nature of these processes may not be readily evident, physically measurable, or even relevant to practical large scale structural analysis. The appearance and manifestation of these dissipative processes, and their influence on the material behavior parameters, are often very sensitive to the conditions which the

specimen is subjected to. In general, this sensitivity is observed to be influenced by: i) the physical dimensions of the structural component as compared to a characteristic material continuum dimension, ii) whether the independent variable of loading is a prescribed boundary traction or a prescribed boundary displacement, iii) the rate at which the prescribed loading is applied, iv) the thermal environment of the material, and v) the chemical environment of the material.

It should be clearly emphasized that while the loading rate will influence the material behavior parameters, this does not necessarily cast any subsequent analysis into an explicitly time dependent form. The quasi-static assumptions of linear and nonlinear analyses still hold. This applies even when the dependence of the material parameters on the type of material test is addressed, as is the case here.

Any model of material behavior for structural component analysis and design will do so through a unique material constitutive relation. This relation, by definition, will address local nonlinearity of the material behavior. Such a relation, however, should be evaluated in a model of an appropriate material test specimen. A material specimen, as already mentioned, may be relatively straightforward to define from theoretical considerations for purely elastic responses. The interpretation of test data for dissipative responses is far more difficult due to the material inhomogeneity of the specimen caused by the loading. This becomes apparent for any appreciable level of global nonlinearity. The effects of specimen size, loading scheme, loading rate, temperature, and environment may individually, or in combination, produce this effect.

For the purposes of this report, attention will be directed toward the effects of specimen size at constant loading rate for stress controlled loading. In general, the concepts and procedures demonstrated here are applicable to a wide range of conditions, which may include differences in loading rate, temperature, or chemical environment.

FINITE ELEMENT MODELING OF CYLINDRICAL TEST SPECIMENS AND THE RELATION TO MATERIAL TESTING

The effects of specimen size and loading rate may be parametrically investigated for a given constitutive relation using the finite element method. Generally, an increase in specimen dimensions is accompanied by a decrease in the specimen ductility, as shown schematically in Figure 6. A specimen size parameter D may be defined from the specimen volume to surface area ratio as

$$D = \frac{V}{A} \quad (17)$$

At a constant value of the size parameter D , an increase in the loading rate also suppresses ductile behavior of the specimen. This is shown schematically in Figure 7.

It should be noted that quantities such as the ultimate stress σ_u and ultimate strain ϵ_u , which coincide with the final fracture of the specimen, are often used to characterize a material's resistance to fracture. The fact that energy is dissipated during the fracture process leads one, more correctly, to define the strain energy required to produce fracture in the specimen as the quantity relevant to material behavior and to the fracture process. The previous discussion of the strain energy density theory, as applied to both macrocrack propagation and microdamage, addresses fracture toughness at the continuum scale in detail through the use of the critical strain energy density $(\Delta W/\Delta V)_c$.

In light of these comments, it should also be noted that the strain energy density at yield, i.e. $(\Delta W/\Delta V)_y$, is in general observed to increase with increasing rate of loading. This is, of course, related to the manner

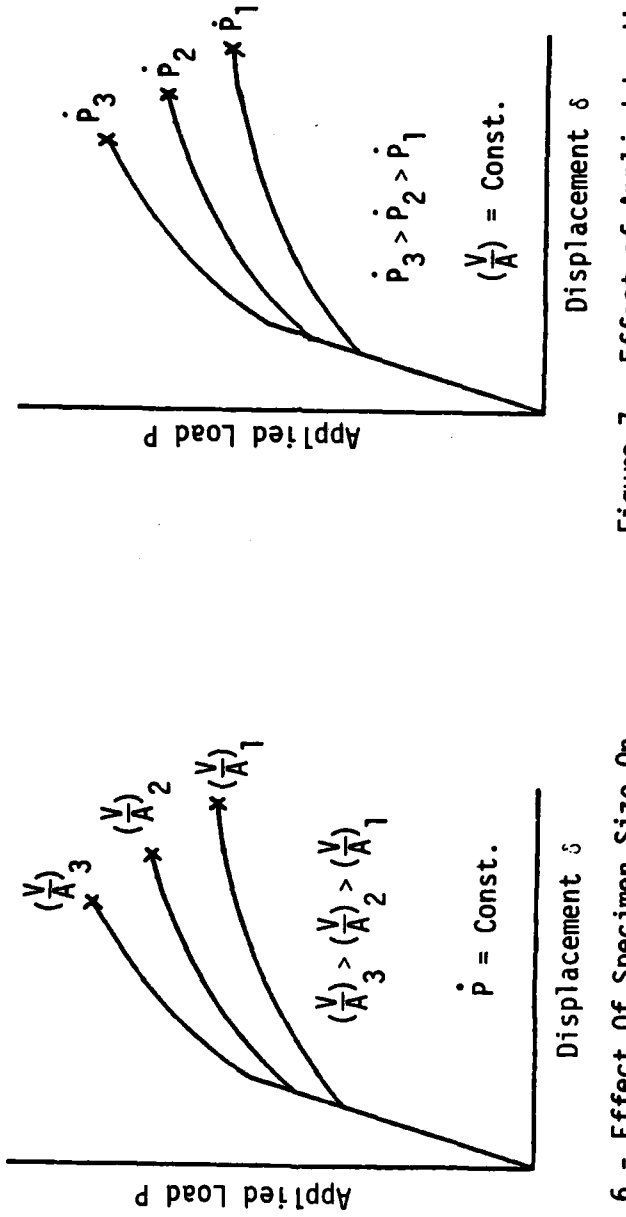


Figure 6 - Effect Of Specimen Size On Load-Displacement Response

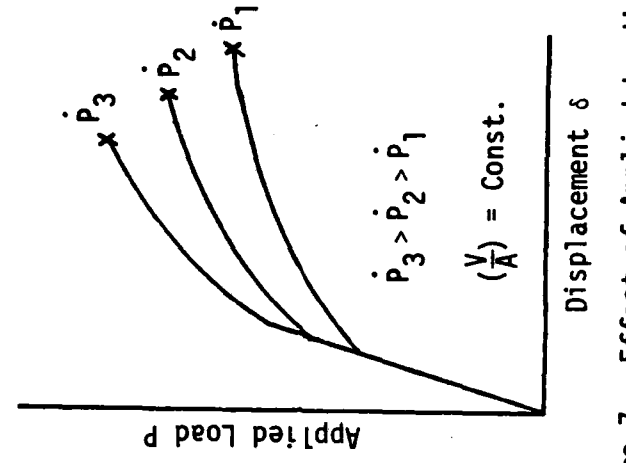


Figure 7 - Effect of Applied Loading Rate On Load-Displacement Response

in which mechanisms below the continuum scale are able to dissipate energy. For similar reasons, the critical value of strain energy density is seen to decrease for higher loading rates. The intermediate energy densities between $(\Delta W/\Delta V)_y$ and $(\Delta W/\Delta V)_c$, for a given set of test conditions, provides an envelope of material behavior whose role in global response and macrocrack growth must be addressed (Figure 8).

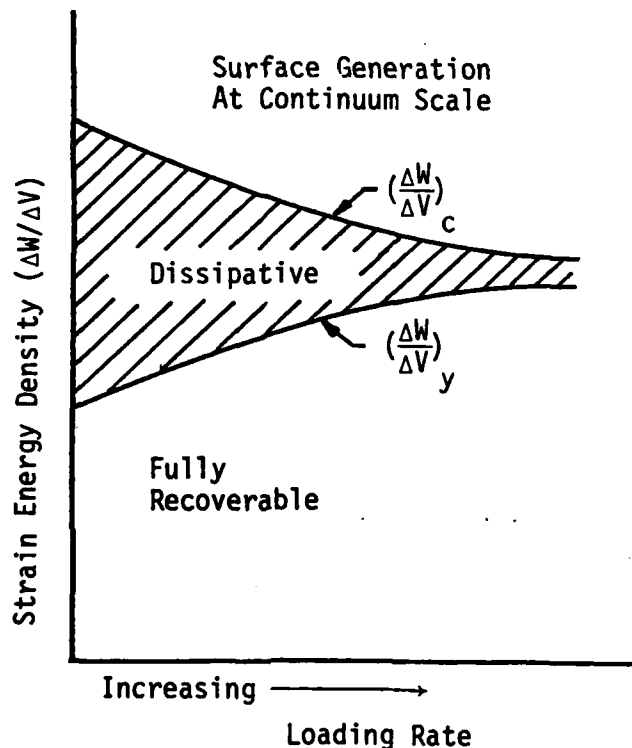


Figure 8 - Typical Response Regimes Of Material Element To Strain Energy Density

A compressive test program to characterize the influence of size and rate effects on the material behavior and strain energy density function would identify: i) the sensitivity of the material to the specimen size and specimen loading rates representative of those expected in service, ii) evaluate the material constitutive relation, and iii) quantify this dependence for the designer.

Consider, for example, the evaluation of a particular material (described by an appropriate constitutive law) using nine individual tensile tests. Three different specimen sizes would each be tested at three different loading rates, for the total of nine tests. The load-displacement responses of the specimens would be influenced by the size of the nucleated macrocrack, the crack growth increments and the material damage below the continuum scale prior to global instability of the specimen.

In order to demonstrate the effect of local material inhomogeneity on specimen global response, a finite element simulation of three uniaxial tensile specimens was performed. All three specimens were assumed to be of the same material, with the constitutive relation shown in Figure 9, but of different sizes. For simplicity, they will be referred to as small, medium, and large. All external specimen dimensions are scaled proportionally as 3: 4: 5 and are shown in Figure 10. Each cylindrically shaped specimen had a diameter-to-length ratio of 2.0, which was found to adequately represent the remote constant stress loading condition at the upper and lower boundaries for inhomogeneity in the center of the specimen. This eliminated the necessity of including the threaded portion of such a specimen in the analysis, which would have significantly increased the overall computational requirements.

As is commonly observed from tensile specimens loaded to fracture, a circular macrocrack will coalesce internally in the specimen, perpendicular to the specimen axis. The transition of a continuum region from a crack free zone to a zone with an initiated crack is not well understood. With this deficiency, the process is difficult to include in an analytical or numerical scheme without the use of some assumptions based on observation. For this

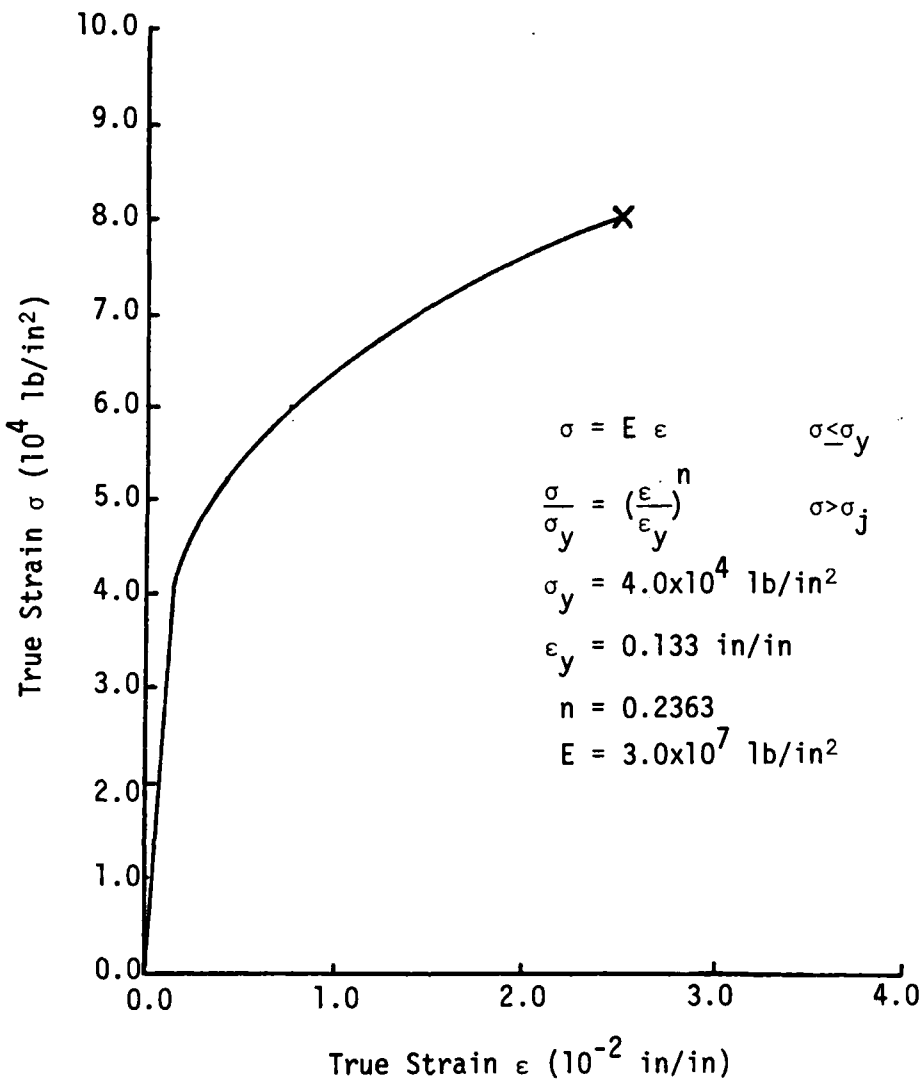
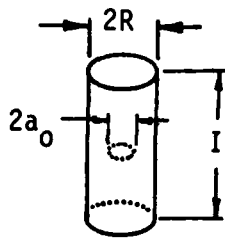


Figure 9 - True Stress - True Strain Relation
For Finite Element Model

analysis, initiation of a macrocrack was assumed to coincide with the onset of nonlinear specimen response. The radius of the initiated crack was taken as 0.1" in all cases.

For the medium sized specimen, the onset of the global nonlinear response was assumed to occur when the average applied stress was equal to the yield

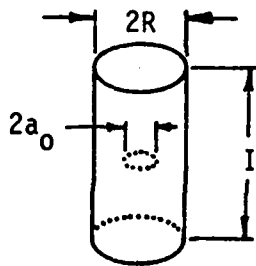


Small Specimen

$$R = 0.3"$$

$$H = 0.6"$$

$$a_0 = 0.1"$$

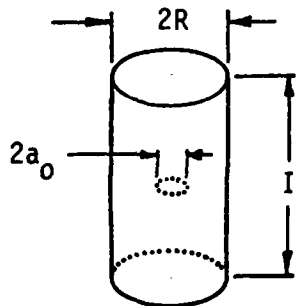


Medium Specimen

$$R = 0.4"$$

$$H = 0.8"$$

$$a_0 = 0.1"$$



Large Specimen

$$R = 0.5"$$

$$H = 1.0"$$

$$a_0 = 0.1"$$

Figure 10 - Axisymmetric Test Specimens

point of the constitutive relation. For the material under consideration the yield stress was 40,000 lb/in². The onset of global nonlinearity in the large and small sized specimens was assumed to occur at 45,000 and 35,000 psi, respectively. This assumption reflects the suppressed and enhanced ductility

attributable to the effect of specimen size. Finite element grids for each of the three specimen geometries are shown in Figures 11, 12, and 13. All elements are 12 node, cubic displacement, isoparametric elements. The initiation crack size of 0.1" is identical for all specimens as discussed above, as is the grid in the immediate vicinity of the crack. From the axisymmetric nature of the specimen, only one quadrant of a diametrical cross section is necessary for each finite element model. A total of 73 elements were used in the small size specimen grid, with 411 nodes. For the medium size specimen 79 elements and 444 nodes were used, while for the large size specimen, 85 elements and 477 nodes were used.

The Axisymmetric/Planar Elastic Structures (APES) fracture mechanics and stress analysis finite element program [5] performed the stress analysis portions of each load increment. The $r^{1/2}$ displacement filed in the immediate vicinity of the crack tip is embedded in the solution through the use of 1/9 and 4/9 nodal spacing on the element sides adjacent to the crack tip. The CDC 6400 computer used in this investigation required between 190 and 215 system seconds and 160k of central memory to complete the stress analysis at each point in the incremental analysis for a given specimen load and damage distribution.

The microdamage processes that occur in the material manifest themselves by changes in the material properties at the continuum level. The finite element formulation allows for this by associating with each element one of 25 different material property pairs (i.e. elastic modulus E and Poisson's ratio v). The set of properties (E_1, v_1) corresponding to the initial elastic behavior of the material, while 24 discrete material property pairs (E_i, v_i) or $i = 2, 3, 4, \dots, 24$ correspond to different stages of damaged material.

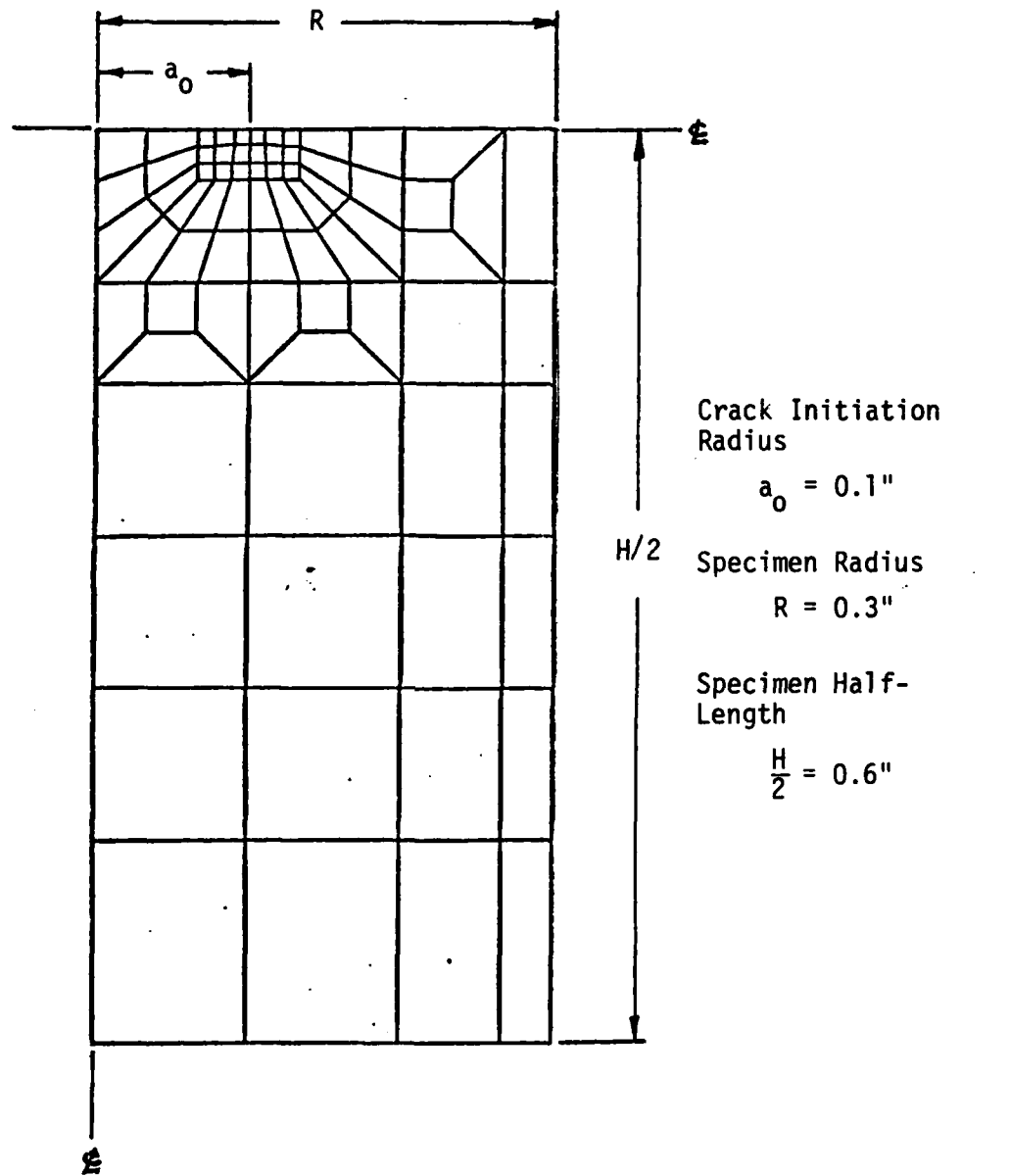


Figure 11 - Small Size Axisymmetric Specimen Finite Element Grid

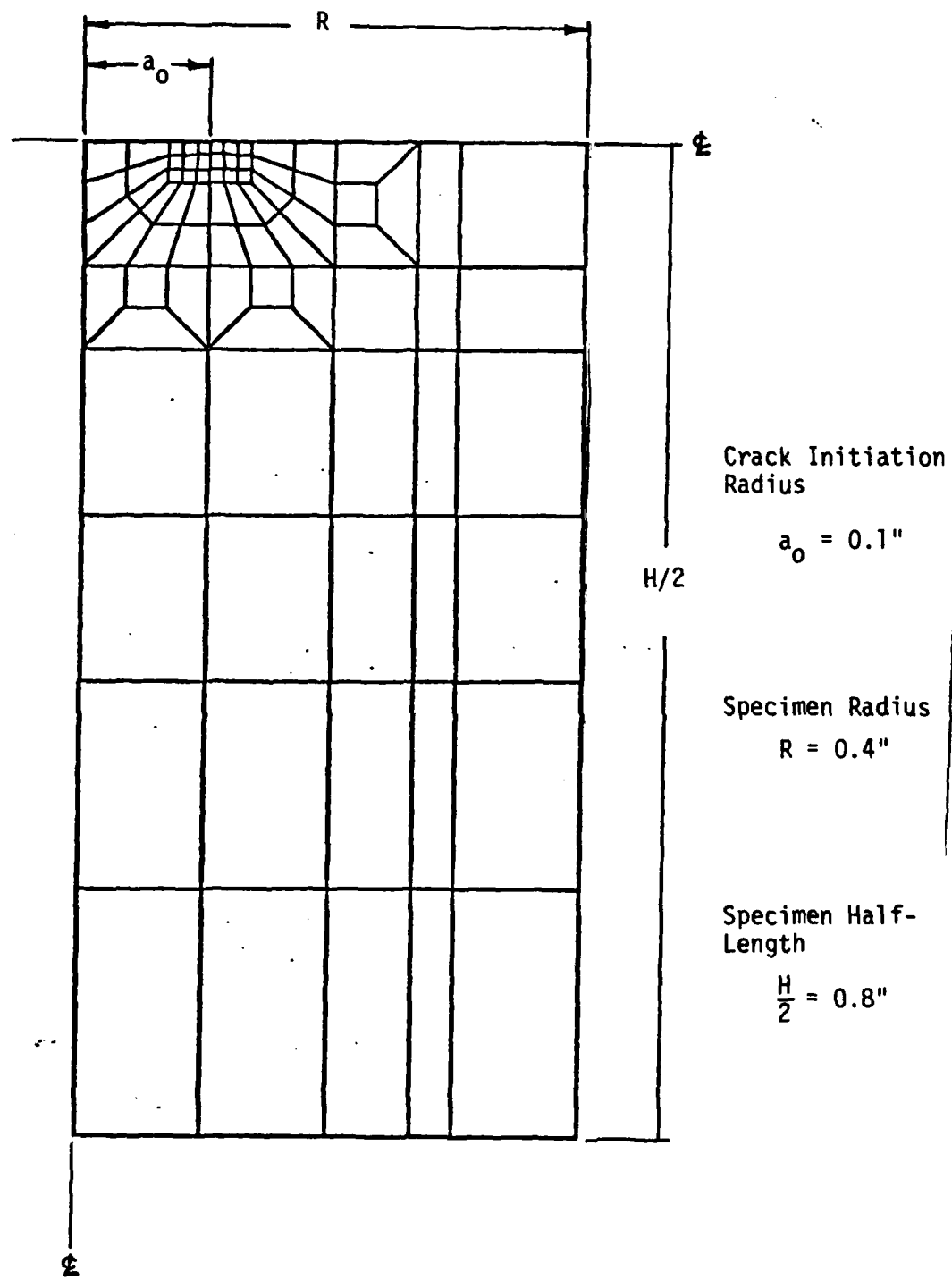


Figure 12 - Medium Size Axisymmetric Specimen Finite Element Grid

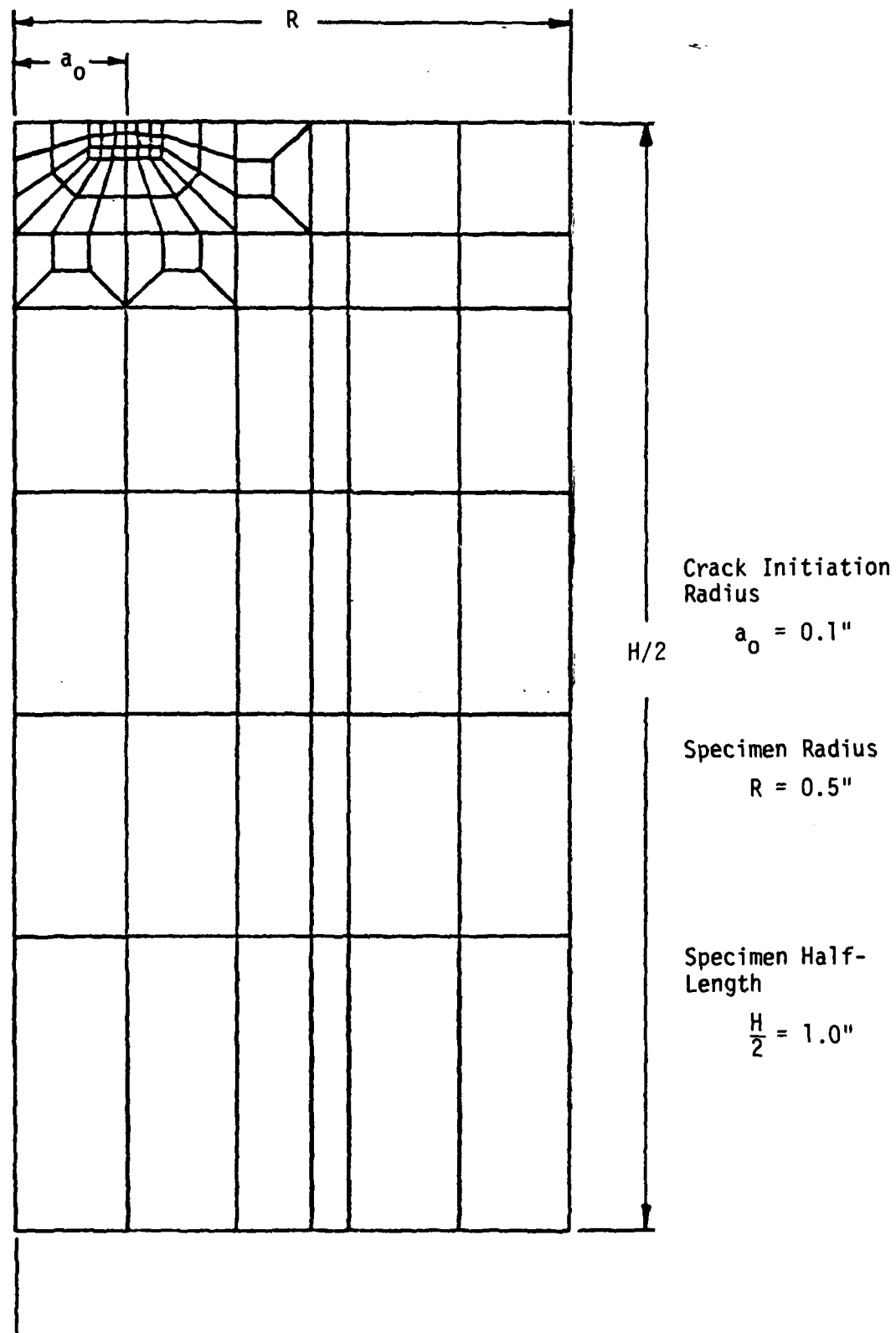


Figure 13 - Large Size Axisymmetric Specimen Finite Element Grid

The extension of the macrocrack in the specimen, as determined by the crack growth criteria, is incorporated into the finite element model by a uniform expansion of the crack zone shown schematically in Figure 14. The dimensions of this zone boundary expand in proportion to the percentage growth of the macrocrack, within the confines of the overall grid boundary. The remaining element sizes are decreased to preserve the external specimen dimensions. Small changes in the damage zone will occur from this algorithm. However, since crack growth increments are typically less than 10% of the current crack length, the effect of this on the global specimen response will be negligible. Crack instability will occur, in the context of the discretization when the lowest value of $(\Delta W/\Delta V)_c^*$ is reached in the element ahead of the crack tip.

Using the concepts and procedures outlined above, the total load P versus surface displacement δ responses of the three specimens are shown in Figure 15. The failure loads of the small, medium, and large size specimens are 15000, 27600, and 44800 pounds, respectively. The nonlinearity of the responses are, of course, generated by the effects of nonlocalized, low intensity damage away from the crack, higher intensity damage in enclaves near the crack periphery, and the crack growth itself.

The load-displacement response of each of the three tensile specimens was converted into an applied true stress - true strain response. Use of the axial displacement δ of the exterior surface farthest from the crack plane was consistent with traditional methods of defining strain. These results are shown in Figure 16.

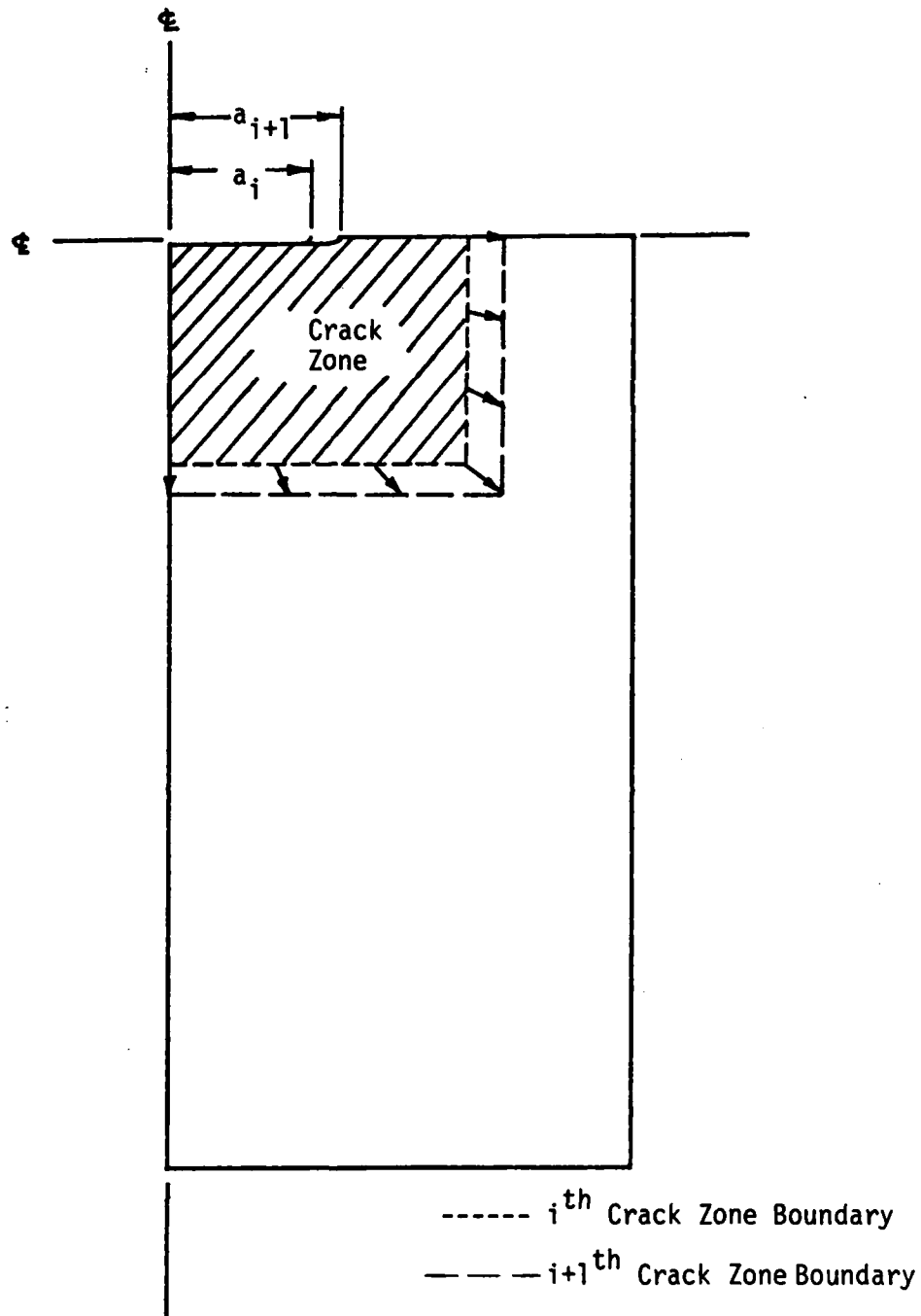


Figure 14 - Finite Element Grid Convection
For Axisymmetric Specimen
Series

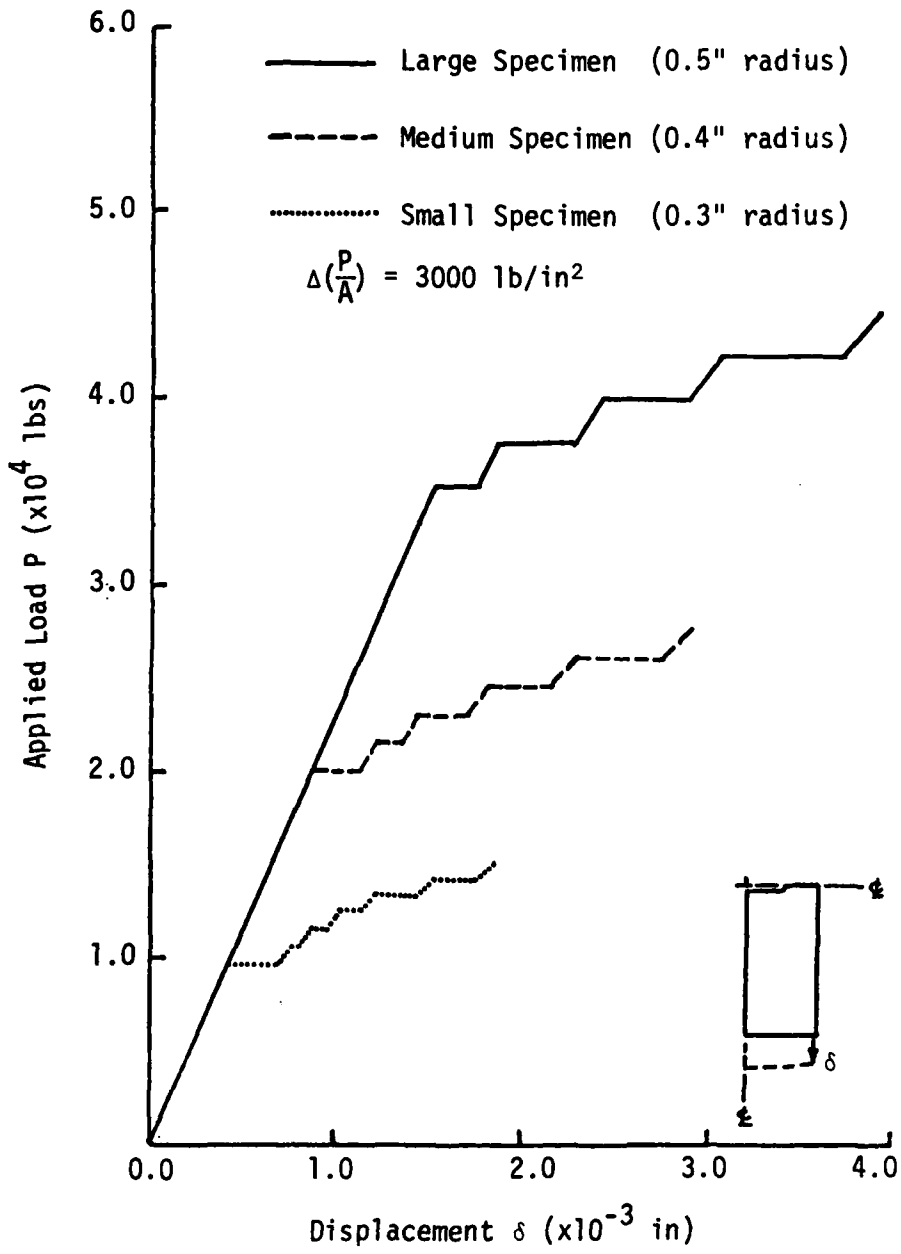


Figure 15 - Applied Load Versus Surface Displacement
For Three Specimen Sizes

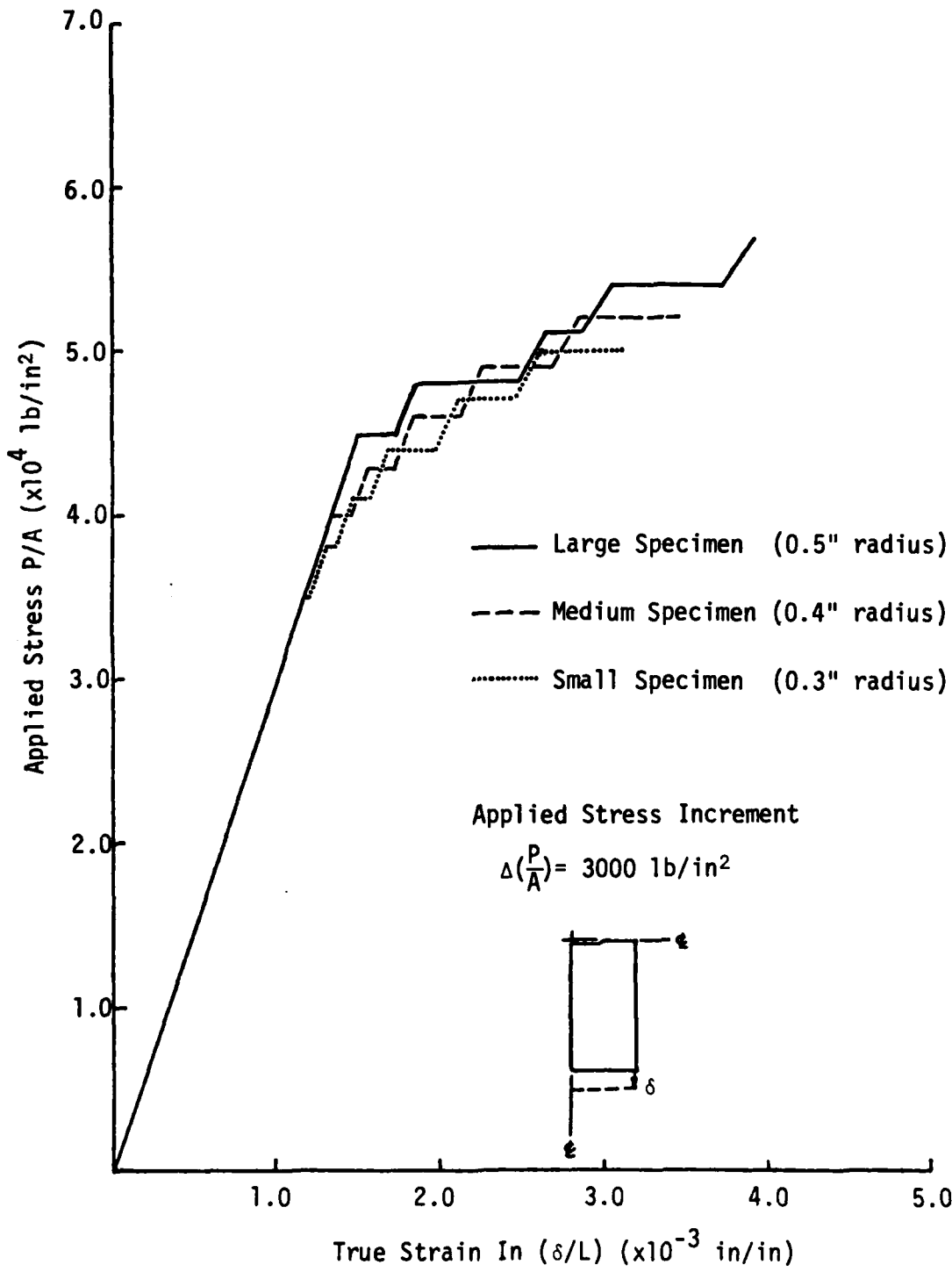


Figure 16 - Applied Stress Versus True Strain Response For Three Specimen Sizes

The large specimen is clearly departing from a linear response in a more dramatic manner than either the medium or small sized specimen. This is due to two factors. First, the large specimen macrocrack is initiated at a higher load. The macrocrack propagation will be enhanced by this fact. Second, the intensity of the microdamage will significantly reduce the value of the relative critical strain energy density. This further enhances crack growth and reduces the local material stiffness throughout the specimen.

The response of the medium specimen, as compared to the small specimen, exhibits the same type of behavior, but to a lesser degree. Due to the difference in the applied loads corresponding to the onset of nonlinearity, the overall reduction in stiffness of the two specimens will be likewise suppressed.

The plots of strain energy density $\Delta W/\Delta V$ versus distance ahead of crack tip are given in Figures 17, 18 and 19 for the three specimen sizes. The current value of relative critical strain energy density $(\Delta W/\Delta V)_c^*$, reflecting on the intensity of material damage ahead of the crack, is also shown at each loading increment for crack propagation. The intersection of $\Delta W/\Delta V$ and $(\Delta W/\Delta V)_c^*$ yields the increment of crack growth.

The relative strain energy density factor S^* is plotted against the crack growth increment Δa in Figure 20 as calculated from Equation 15. Since the intensity of material damage ahead of the crack tip is changing, the value of $(\Delta W/\Delta V)_c^*$ will, in general, be different for each crack growth increment. This results in non-self-similar growth of the combined crack and damage zone. The nonlinear nature of S^* versus Δa is an indication of this

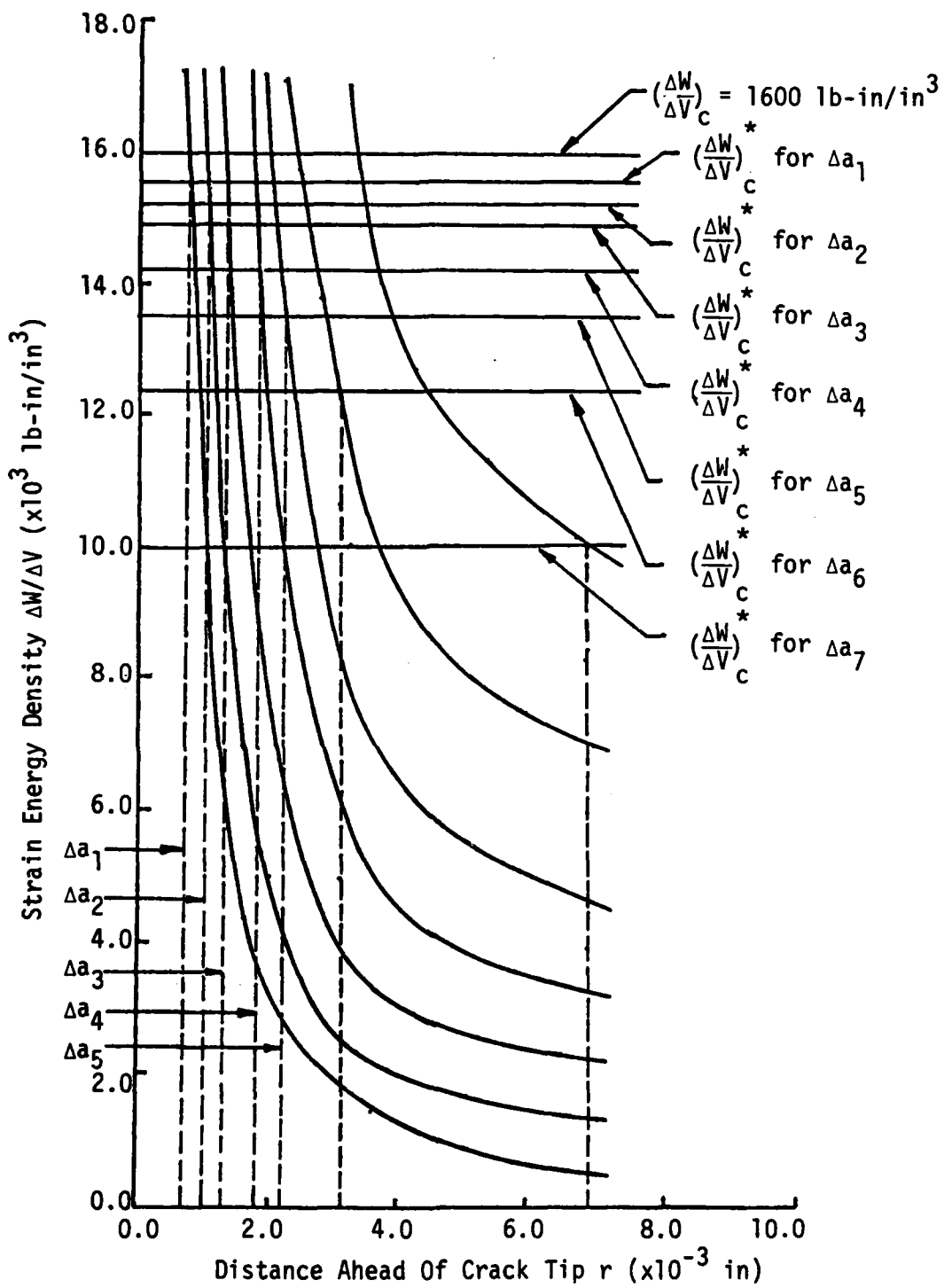


Figure 17 - Strain Energy Density Ahead Of Crack Tip For Medium Specimen

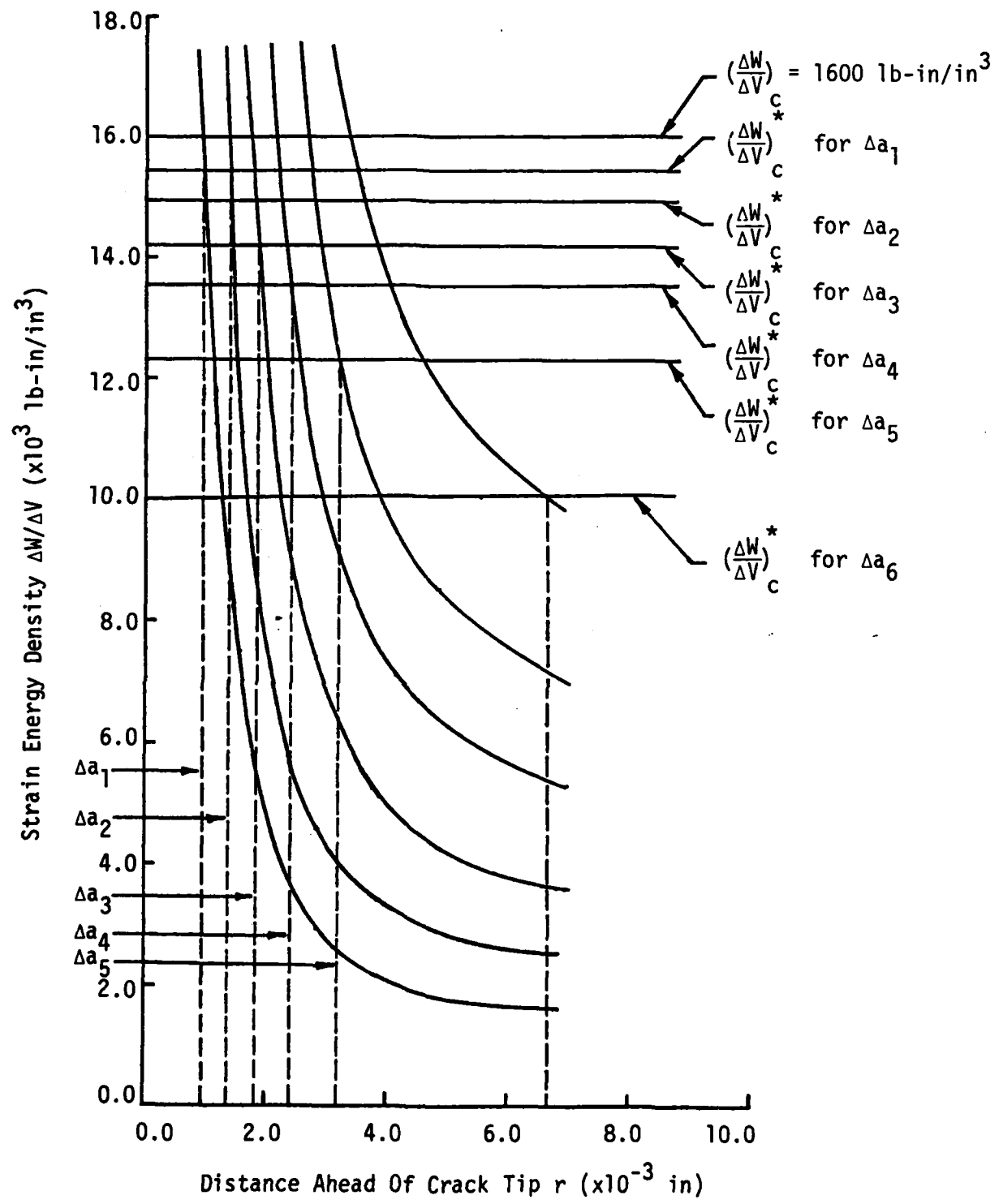


Figure 18 - Strain Energy Density Ahead Of Crack Tip For Medium Specimen

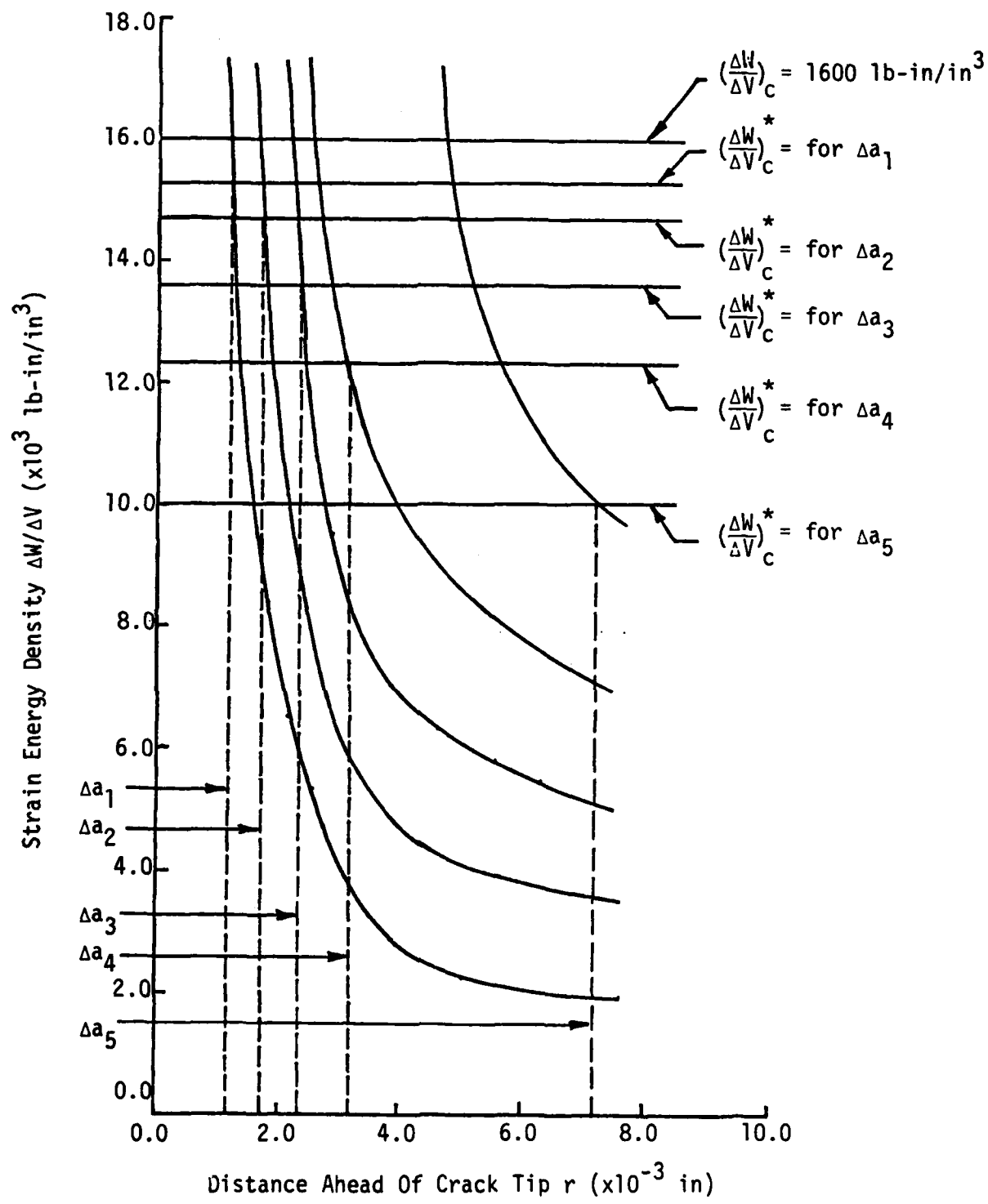


Figure 19 - Strain Energy Density Ahead Of Crack Tip For Large Specimen

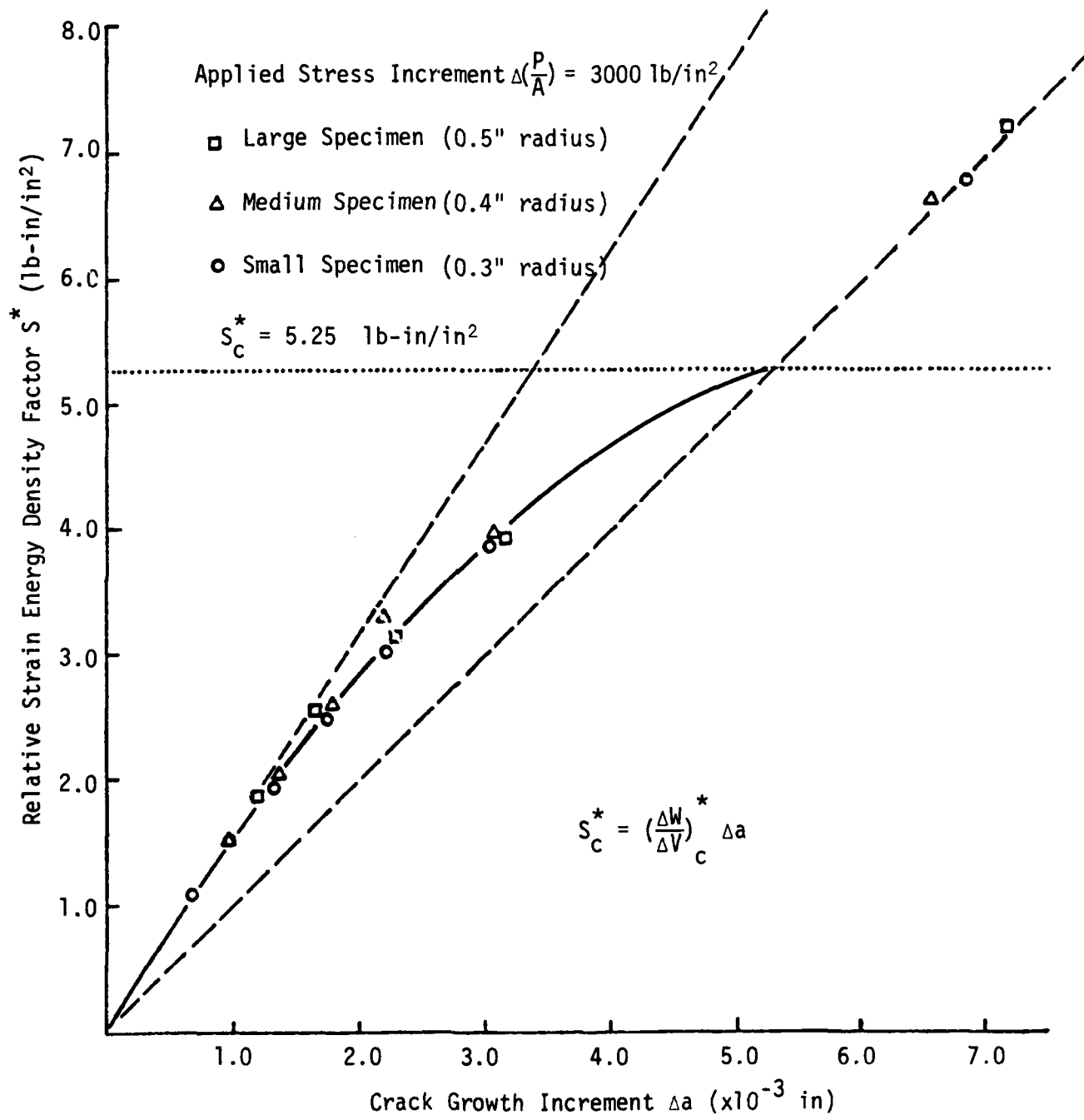


Figure 20 - Relative Strain Energy Density Factor Versus Crack Growth Increment For Three Specimen Sizes

fact. The curves generated by each of the three specimen sizes, however, clearly are one and the same. This leads to the observation that the evolution of the crack into material of any damage intensity (within the bounds of possible material behavior) may be described by such a curve.

From the crack growth increments predicted by the finite element analyses, the strain energy density factor S can be calculated from Equation (15). The plot of S versus the increment of crack growth Δa , for all three specimens, clearly indicates the linear relationship of these two quantities for the given material (Figure 21). All three lines are coincident, identifying the S versus Δa curve as being unique to crack growth in this material at the prescribed loading rate regardless of specimen size.

The relative strain energy density factor S^* versus crack growth $a-a_0$ (or crack length a) is nonlinear for each specimen size (Figure 22). The effect of specimen size is evident by the relative shift to higher values of S^* for larger specimen sizes. Final instability of the crack coincides with the abrupt change in behavior of the final data points for each of the three specimens. Each of these three points coincides with the final increment of crack growth into material at the limiting intensity of damage governed by the true stress - true strain curve.

The relation of the strain energy density factor S versus crack growth $a-a_0$ (or crack length a) is shown in Figure 23. The linear nature of S versus a is apparent. The effect of specimen size results in a relative shift of the lines toward higher values of S for larger specimen sizes. Crack instability is also accompanied by points whose location differs significantly from their expected location on the S versus $a-a_0$ line corresponding to stable growth.

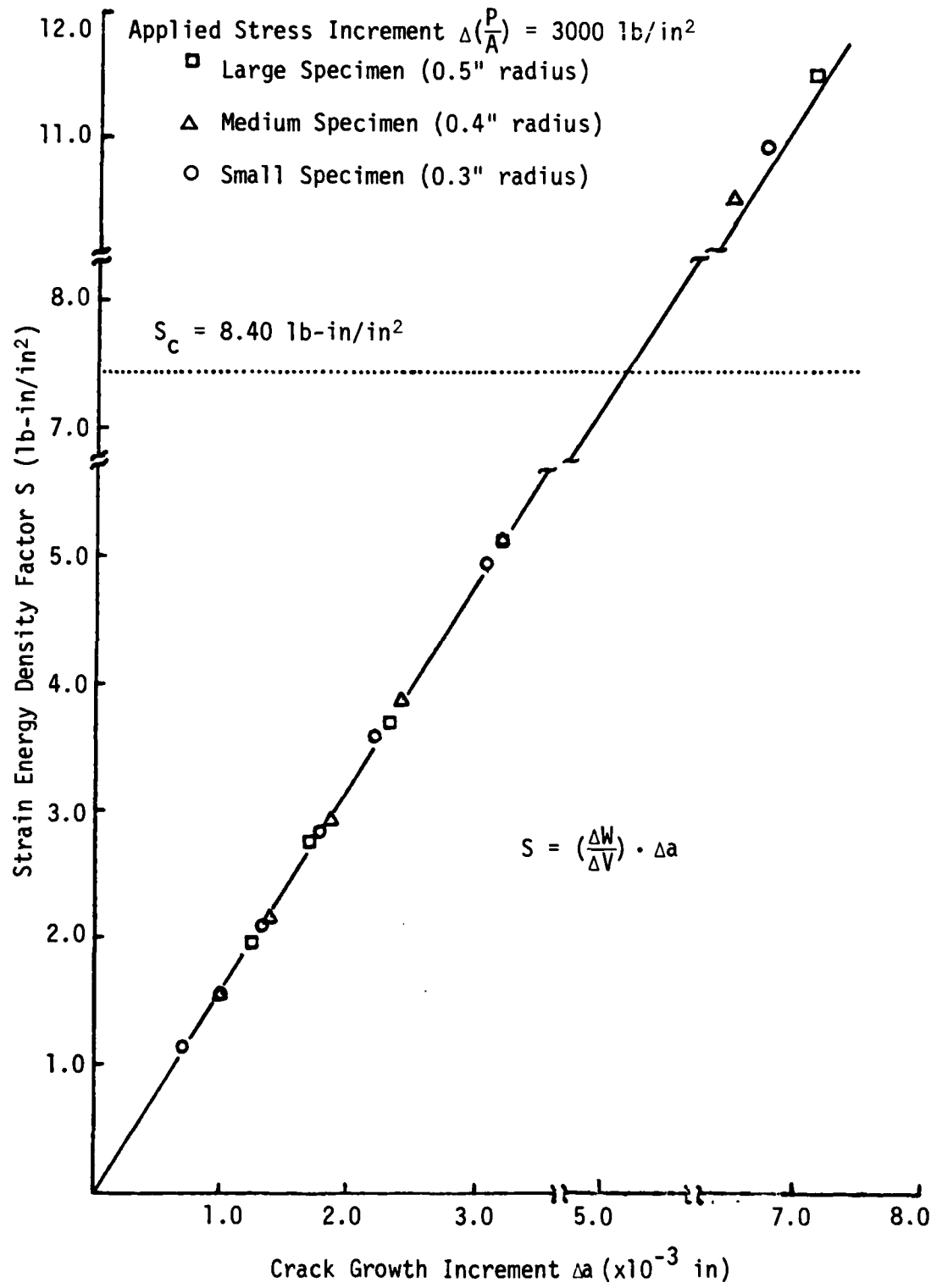


Figure 21 - Strain Energy Density Factor Versus Crack Growth Increment For Three Specimen Sizes

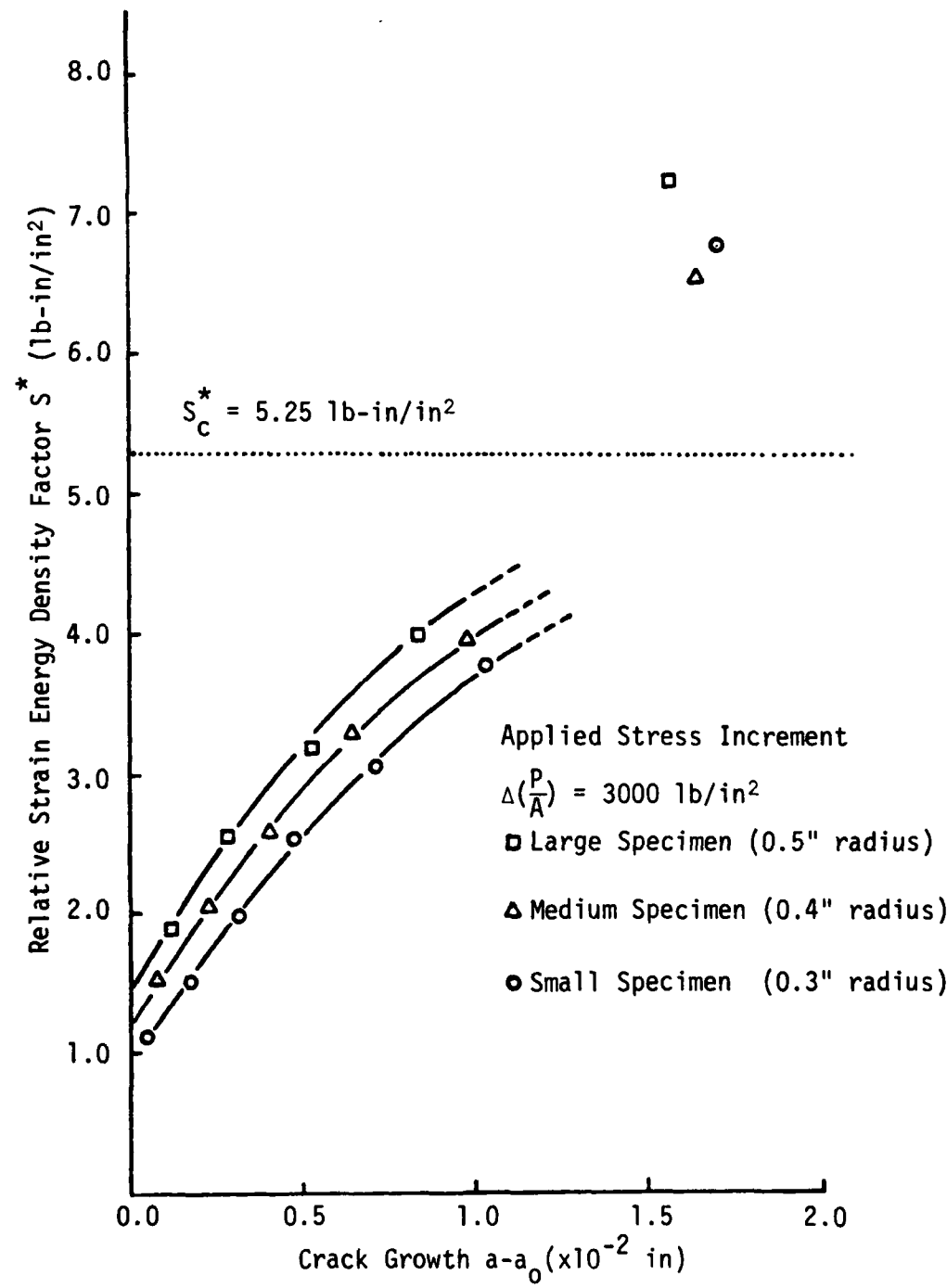


Figure 22 - Relative Strain Energy Density Factor Versus Crack Growth For Three Specimen Sizes

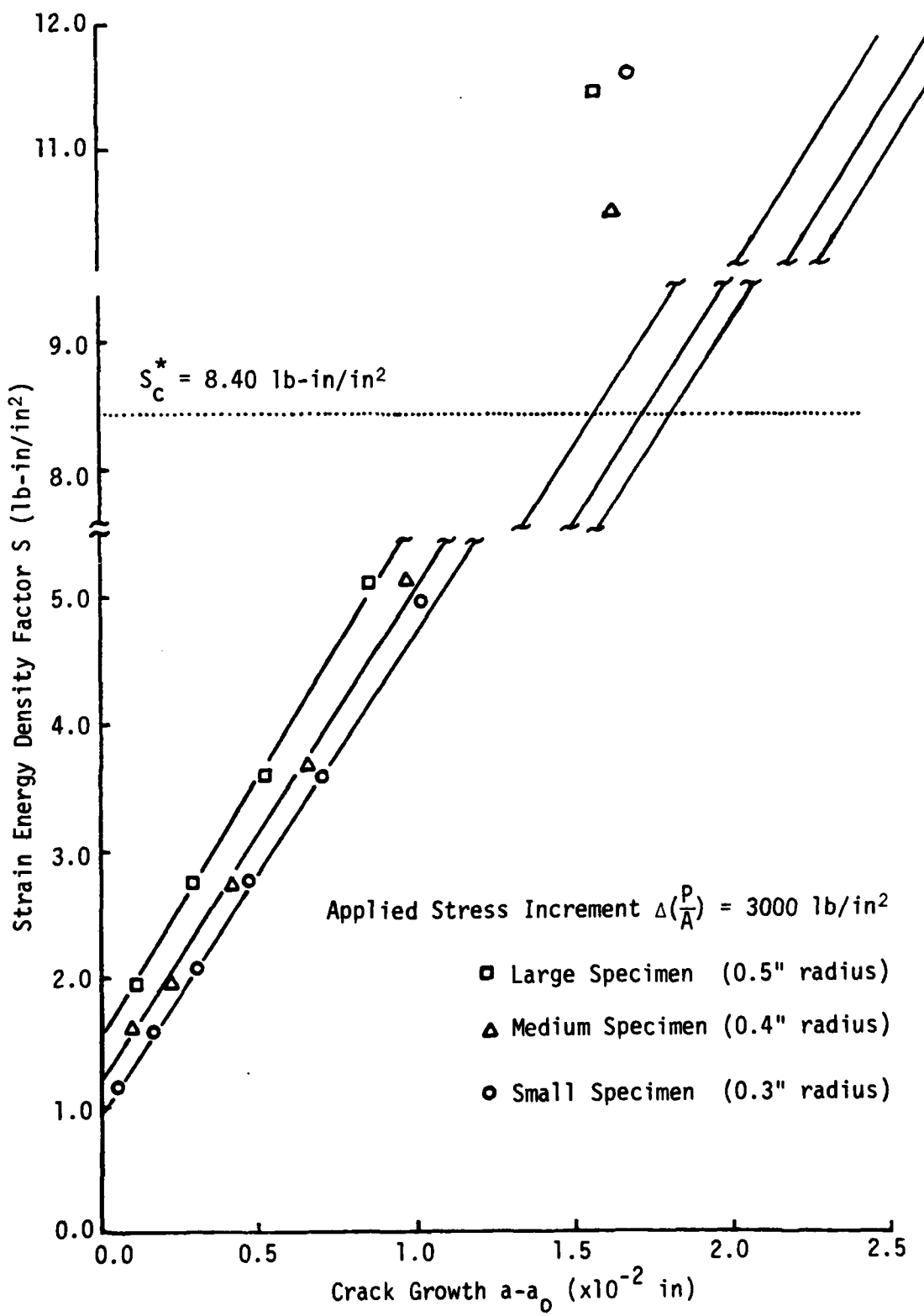


Figure 23 - Strain Energy Density Factor Versus Crack Growth For Three Specimen Sizes

The crack growth $a_c - a_0$, corresponding to specimen instability, was calculated to be 16.9, 16.4, and 15.6% of the initiation crack length a_0 for the small, medium, and large specimens. The influence of increasing specimen size leads to less total crack growth $a - a_0$, despite the larger growth per increment Δa , because fewer load increments are required to reach instability.

The critical value of the relative strain energy density factor S^* may be estimated from the intersection of the nonlinear S^* versus Δa curve and the straight line of slope $\min (\Delta W/\Delta V)_c^*$. This is shown in Figure 20. $\min (\Delta W/\Delta V)_c^*$, as discussed before, corresponds to the lowest value of material toughness described by the constitutive relation. The final calculated increment of crack growth and final load are always slightly greater than or equal to the values necessary for incipient crack instability. This implies that some measure of overload has been imparted to the specimen, providing slightly more than the minimum energy required for instability.

For the material used in this investigation, S_c^* is estimated to be 5.25 lb-in/in². From Equation (15), the value of S_c is calculated to be 8.40 lb-in/in², and is shown in Figure 21.

CONCLUDING REMARKS

This sample set of calculations has shown how the strain energy density concept may be used to address material damage and macrocrack propagation in the framework of a single consistent criterion based on the strain energy density behavior of the material. Finite element analyses of post-yield behavior, accompanied by macrocrack initiation and a period of stable crack growth, has demonstrated the application of the model in the case of three geometrically similar brittle-elastic specimens of different sizes. The results of this study have shown how traditional methods of reducing load-displacement data to a stress-strain representation are inadequate. The difficulty of determining a unique material constitutive relation from such data, in light of material inhomogeneity within the specimen during post-yield behavior and the effects of specimen size, is apparent.

It should be noted that the magnitude of the load increment serves to translate changes in the applied loading rate to the amount of stable crack growth generated at the crack tip. The material constitutive law will be relatively insensitive to the changes in loading rates considered away from the crack tip. The relative rate at which energy is introduced into the material within the core region will not, of course, be proportional to that away from the crack tip. The applied loading rate as well as the growth rate of the crack itself contribute to this effect. The net effect of moderate increases in the remote applied loading rate is to advance the rate at which material toughness decreases near the crack tip. This accelerates the crack growth process, but over a smaller range of applied load defined from the onset of global nonlinearity to global instability. The influence of the load

increment size is currently being studied.

Failure, for the purposes of this investigation, has been defined as the unstable generation of surface area by crack propagation. This may be too liberal of a condition for a particular practical application. It does, however, represent an upper limit on the geometric integrity of the component. A subsidiary condition of failure may, of course, be defined. Excessive deformation is an example of such a definition which may be useful when large scale ductility is predicted for the specimen. The utility of the strain energy density criterion lies in its ability to provide the designer with information on the global crack growth and final instability as well as a broad spectrum of measures quantifying component performance. The practical capability to estimate critical loads corresponding to different definitions of failure (from a single yield-to-global fracture instability analyses) is a powerful tool not featured by theories able to address only particular failure modes or employing restrictive assumptions on material behavior.

BIBLIOGRAPHY

- [1] Sih, G. C., "A Special Theory of Crack Propagation", Methods of Analysis and Solutions of Crack Problems, ed. by G. C. Sih, Noordhoff International Publishing, pp. XXI-XLV, 1973.
- [2] Sih, G. C., "Some Basic Problems in Fracture Mechanics and New Concepts", Engineering Fracture Mechanics, 5, pp. 365-377, 1973.
- [3] Sih, G. C. and Matic, P., "Mechanical Response of Materials with Physical Defects, Part 1: Modeling of Material Damage for Center Cracked Panel", Institute of Fracture and Solid Mechanics Technical Report AFOSR-TR-81-1, 1981.
- [4] Sih, G. C. and Matic, P., "Mechanical Response of Materials with Physical Defects, Part 2: Combined Modeling of Material Damage and Crack Propagation for Center Cracked Panel", Institute of Fracture and Solid Mechanics Technical Report AFOSR-TR-82-2, 1982.
- [5] Hilton, P. D., Gifford, L. N. and Lomack, O., "Finite Element Fracture Mechanics of Two Dimensional and Axisymmetric Elastic and Elastic-Plastic Cracked Structures", Naval Ship Research and Development Center Report No. 4493, 1975.

END

FILMED

10-83

DTIC